

See discussions, stats, and author profiles for this publication at: <https://www.researchgate.net/publication/47280127>

# RmlC, a C3' and C5' carbohydrate epimerase, appears to operate via an intermediate with an unusual twist boat conformation

ARTICLE · JANUARY 2007

Source: OAI

CITATIONS

8

READS

22

12 AUTHORS, INCLUDING:



**Changjiang Dong**

University of East Anglia

36 PUBLICATIONS 1,430 CITATIONS

SEE PROFILE



**Joseph S Lam**

University of Guelph

191 PUBLICATIONS 5,650 CITATIONS

SEE PROFILE



**Robert A Field**

John Innes Centre

241 PUBLICATIONS 4,654 CITATIONS

SEE PROFILE



**James Henderson Naismith**

University of St Andrews

219 PUBLICATIONS 7,285 CITATIONS

SEE PROFILE

# RmlC, a C3' and C5' Carbohydrate Epimerase, Appears to Operate *via* an Intermediate with an Unusual Twist Boat Conformation

Changjiang Dong<sup>1†</sup>, Louise L. Major<sup>1†</sup>, Velupillai Srikanthasasan<sup>1†</sup>  
James C. Errey<sup>2</sup>, Marie-France Giraud<sup>1</sup>, Joseph S. Lam<sup>3</sup>  
Michael Graninger<sup>4</sup>, Paul Messner<sup>4</sup>, Michael R. McNeil<sup>5</sup>  
Robert A. Field<sup>2</sup>, Chris Whitfield<sup>3</sup> and James H. Naismith<sup>1\*</sup>

<sup>1</sup>Centre for Biomolecular Sciences, The University of St. Andrews KY16 9ST UK

<sup>2</sup>School of Chemical Sciences and Pharmacy, University of East Anglia, Norwich NR4 7TJ UK

<sup>3</sup>Department of Molecular & Cellular Biology, University of Guelph, Ontario, Canada N1G 2W1

<sup>4</sup>Zentrum für NanoBiotechnologie Universität für Bodenkultur Wien A-1180, Vienna, Austria

<sup>5</sup>Department of Microbiology, Colorado State University, Fort Collins, CO 80523 USA

The striking feature of carbohydrates is their constitutional, conformational and configurational diversity. Biology has harnessed this diversity and manipulates carbohydrate residues in a variety of ways, one of which is epimerization. RmlC catalyzes the epimerization of the C3' and C5' positions of dTDP-6-deoxy-D-xylo-4-hexulose, forming dTDP-6-deoxy-L-lyxo-4-hexulose. RmlC is the third enzyme of the rhamnose pathway, and represents a validated anti-bacterial drug target. Although several structures of the enzyme have been reported, the mechanism and the nature of the intermediates have remained obscure. Despite its relatively small size (22 kDa), RmlC catalyzes four stereospecific proton transfers and the substrate undergoes a major conformational change during the course of the transformation. Here we report the structure of RmlC from several organisms in complex with product and product mimics. We have probed site-directed mutants by assay and by deuterium exchange. The combination of structural and biochemical data has allowed us to assign key residues and identify the conformation of the carbohydrate during turnover. Clear knowledge of the chemical structure of RmlC reaction intermediates may offer new opportunities for rational drug design.

© 2006 Elsevier Ltd. All rights reserved.

\*Corresponding author

**Keywords:** site-directed mutagenesis; X-ray crystallography; drug design; epimerization; enzyme

† C.D., L.L.M. and V.S. contributed equally to this work.

Present address: M.-F. Giraud, Institut de Biochimie et de Génétique Cellulaires du CNRS, Université Victor Segalen, Bordeaux 2, 1 rue Camille Saint-Saëns, F-33 077 Bordeaux cedex, France; M. Graninger, Baxter AG Austria, Uferstr. 15, A-2304 Orth/Donau, Austria.

Abbreviations used: RmlC, dTDP-6-deoxy-D-xylo-4-hexulose 3',5'-epimerase; GME, GDP-mannose epimerase; GMER, GDP-6-deoxy-4-keto-D-mannose epimerase/reductase.

E-mail address of the corresponding author: [naismith@st-and.ac.uk](mailto:naismith@st-and.ac.uk)

## Introduction

Carbohydrates serve not only as energy stores, but are also important structural elements and informational molecules in many organisms.<sup>1</sup> They are distinguished by their density of asymmetric centers and functional groups. The inversion of stereochemistry at the asymmetric centers (epimerization) of carbohydrates is a simple means of creating molecular diversity; the resulting diastereoisomers are chemically distinct. Biology has developed a number of different strategies to accomplish such epimeri-

zation reactions and uses several different classes of enzymes to catalyze this transformation.<sup>2–4</sup>

L-Rhamnose is a 6-deoxyhexose that is commonly found in bacterial glycoconjugates. Neither the sugar, nor the enzymes required for its synthesis are found in humans and the pathway has been validated as a potential therapeutic target in several clinically important systems, including *Mycobacterium tuberculosis*.<sup>5–7</sup> In *Pseudomonas aeruginosa*, L-rhamnose is integral to both the lipopolysaccharide (LPS) core oligosaccharide and O-antigen polysaccharides; chromosomal mutations in the *rmlC* gene of serotype O5 and serotype O6 of *P. aeruginosa* resulted in LPS core truncation and loss of pathogenicity.<sup>8</sup> In *Streptococcus mutans*, rhamnose-containing polysaccharide antigens mediate colonization of tooth surfaces<sup>9</sup> and genetic disruption of the rhamnose pathway prevents bacteria initiating or sustaining an infection.<sup>10</sup> In *M. tuberculosis*, L-rhamnose links the peptidoglycan and arabinogalactan in a unique and complex cell wall structure that is essential for viability.<sup>11</sup>

RmlC (dTDP-6-deoxy-D-xylo-4-hexulose 3',5'-epimerase, EC 5.1.3.13) is the third enzyme of the dTDP-L-rhamnose biosynthetic pathway that converts glucose-1-phosphate to dTDP-L-rhamnose.<sup>12</sup> The pathway requires four enzymes, RmlA, RmlB, RmlC and RmlD, the structures of which have been determined.<sup>13–17</sup> RmlC epimerizes the C3' and C5' positions of dTDP-6-deoxy-D-xylo-4-hexulose making dTDP-6-deoxy-L-lyxo-4-hexulose (Figure 1(a)). The 22 kDa RmlC protein does not require a cofactor. There are now four reports of RmlC structures<sup>15,18–20</sup> and co-complexes have been obtained with dTDP-phenol,<sup>15</sup> dTDP,<sup>18</sup> dTDP-D-glucose<sup>19</sup> and dTDP-D-xylose.<sup>19</sup> The co-complexes of RmlC from *Streptococcus suis* with dTDP-D-glucose and dTDP-D-xylose, respectively, provided experimental evidence for the location of the active site.<sup>19</sup> This study identified a conserved His residue as the base for both epimerization reactions, a conserved Lys residue that stabilizes the intermediate enolate anion and a conserved Tyr that acts as an acid.<sup>19</sup>

GDP-mannose epimerase (GME) and GDP-6-deoxy-4-keto-D-mannose epimerase/reductase (GMER) also catalyze C3', C5' epimerization. As part of this epimerization, both enzymes catalyze NAD-dependent redox chemistry at the C4' position;<sup>21–24</sup> the reactions catalyzed by GME are shown in Figure 1(b). Both GME and GMER are members of the short-chain dehydrogenase (SDR) superfamily of enzymes and share no sequence or structural similarity to RmlC, despite the obvious chemical similarity in the epimerization. In the GME structure a single pair of residues has been identified to function as the acid and base for both epimerizations.<sup>24</sup> A structure with the mono-epimerized product revealed that in GME the carbohydrate ring flip occurs during the first epimerization at C5'.<sup>24</sup> The chemical requirements for proton abstraction and consideration of conformational energy of carbohydrates suggested that GME and by analogy GMER operate on a twist boat structure for the

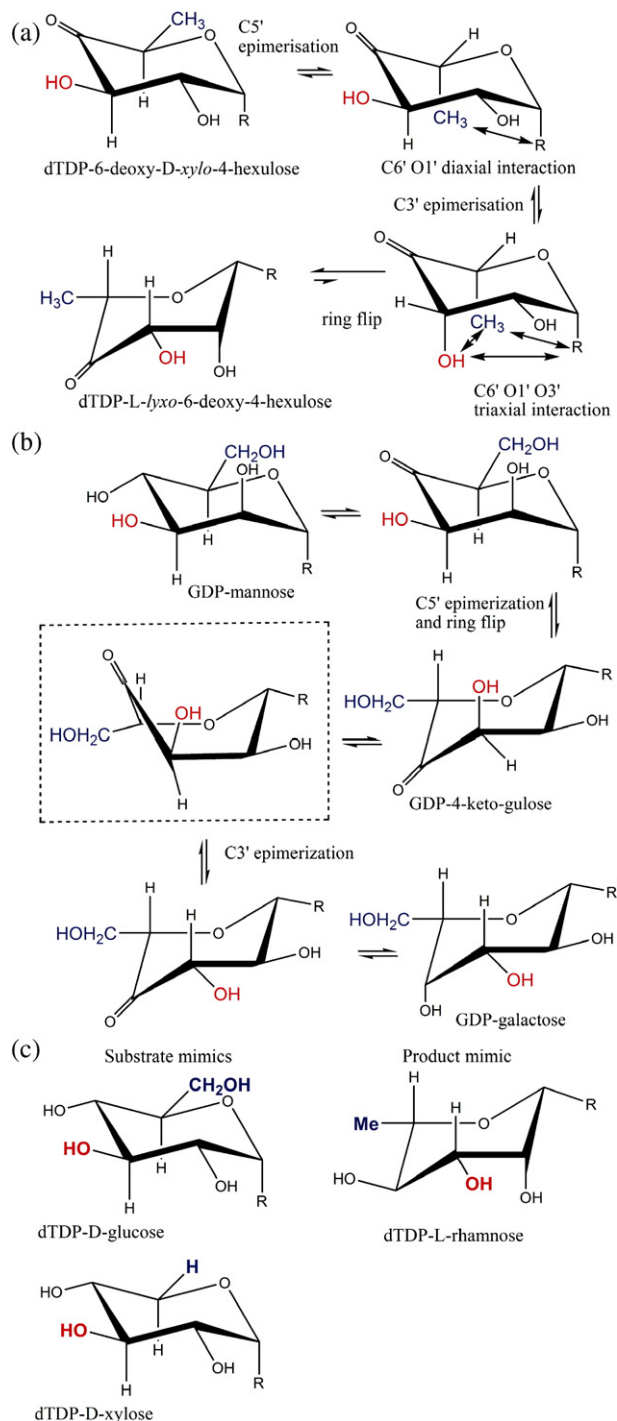


**Figure 1.** (a) R=OdTDP. The RmlC reaction converts dTDP-6-deoxy-D-xylo-4-hexulose to dTDP-6-deoxy-L-lyxo-4-hexulose (thick arrow). This process involves a ring flip as well as epimerization. The steps are shown according to the current convention, however, this route goes through some very high energy intermediates (notably the C1', C3', C5' triaxial product). (b) R=OGPD. The GME reaction converts GDP-D-mannose to GDP-L-galactose. Shown boxed is the predicted twist boat intermediate. The dominant order of the epimerization (C5' first) and the ring flipped form of GDP-L-ribo-4-hexulose were determined experimentally.<sup>24</sup> (c) R=OdTDP. Substrate and product mimics employed in this study.

second epimerization. In light of this we have re-examined RmlC. Since RmlC also carries out a double epimerization, it too faces the same “problem” in the second epimerization. As conventionally written, (Figure 1(a)), the enzyme operates on a very high energy 1, 3, 5 tri-axial intermediate. An alternative would be for the ring to “flip” to relieve the strain. However, the ring flip disrupts the stereochemical requirements for enolate stabilization. For this stabilization, the C–H bond must be orthogonal to the plane of the carbonyl group such that the orbital rehybridization occurs during deprotonation to create an extended (over three atoms) conjugated  $\pi$  system. We have now determined structures of RmlC from *P. aeruginosa*, *S. suis* and *M. tuberculosis* with product mimics (Figure 1(c)). RmlC from *Salmonella enterica* serovar Typhimurium was the first dTDP-6-deoxy-D-xylo-4-hexulose 3',5'-epimerase to be structurally characterized and serves as a prototype. When compared to the *S. enterica* enzyme, RmlC enzymes from *P. aeruginosa* (65% identity), *S. suis* (25% identity) and *M. tuberculosis* (40% identity) show considerable diversity in sequence. The structures of various co-complexes of RmlC from a wide range of organisms suggest that RmlC favors the binding of sugars with an equatorial configuration at the anomeric position. We have measured rates of deuterium incorporation and our data indicate C5' (in the enzyme) is more acidic than C3'. These data suggest that despite the complete lack of similarity in structure and sequence, common epimerization mechanisms are shared between RmlC and GME. This is an example where the common chemical requirements of a transformation drive the convergent evolution of the enzyme mechanisms.

## Results

### *P. aeruginosa* RmlC structure with dTDP-xylose

The structure of RmlC from *P. aeruginosa* contains 184 amino acid residues, consisting of the whole RmlC (residues Met1 to Pro181) plus part of the His-tag linker (Ser-Met-Ser); the remainder of the N-terminal His-tag is disordered. The structure is essentially identical to those described previously, containing 13  $\beta$ -strands that form a sandwich. One  $\beta$  sheet is crucial for forming a dimer interface (Figure 2(a)). The changes in the proteins resulting from binding of nucleotide have been described in detail.<sup>15,19</sup> In the dTDP-D-xylose complex the carbohydrate ring is not found at the active site and only a portion of the ligand is observed (Figure 3(a)). We obtained a similar result with dTDP-D-glucose (data not shown); however the crystals were of lower resolution. The  $\alpha$ -phosphate of the sugar nucleotide is anchored to the protein by salt contacts and by bridging water molecules to the protein *via* the same interactions observed for dTDP-D-glucose, dTDP-D-xylose complexes of *S. suis*<sup>19</sup> and for the

dTDP complex of RmlC from *Methanobacterium thermoautotrophicum*<sup>18</sup> (Figure 2(b)). However, in both monomers the  $\beta$ -phosphate is twisted out of its normal binding site (Figure 2(b)) and the  $\beta$ -phosphate has a significantly higher *B*-factor ( $>10 \text{ \AA}^2$ ) than the  $\alpha$ -phosphate, consistent with disorder of the carbohydrate. This twisting out of the normal binding site suggests that the sugar ring is not recognized by the protein/ HPLC analysis of the nucleotide and sugar nucleotide content of *P. aeruginosa* RmlC:dTDP-xylose crystals reveals only a very small amount of dTDP compared to dTDP-xylose. This establishes dTDP-xylose is indeed present in the crystal structure and hence must be disordered. At the active site in one monomer there is some weak density that is consistent with a tartrate molecule (Figure 3(a)); in the other monomer the tartrate density is less distinct. Tartrate does not appear to inhibit the enzymes in our assays. In the *S. suis*<sup>19</sup> enzyme E78 makes a bidentate hydrogen bond with dTDP-glucose and dTDP-xylose. The Glu residue is not conserved, nor is the structure of the loop containing E78<sup>19</sup> conserved in other RmlC enzymes.

### *P. aeruginosa* RmlC structure with product

To probe the nature of RmlC substrate binding we incubated the *P. aeruginosa* enzyme with the authentic substrate dTDP-6-deoxy-D-xylo-4-hexulose. Since the substrate is chemically labile, we chose the *P. aeruginosa* enzyme for these experiments as it crystallizes closer to neutral pH, where the keto sugar is more likely to remain intact. Although the complex was crystallized in tartrate, the sugar ring is bound at the enzyme active site. This observation is in contrast to both the dTDP-D-glucose and dTDP-D-xylose complexes of the *P. aeruginosa* enzyme. The density clearly shows that the sugar has an equatorial linkage to the nucleotide and indicates a distorted chair consistent with a keto function (Figure 3(b)). The density is consistent with the product dTDP-6-deoxy-L-lyxo-4-hexulose rather than substrate or monoepimerized product bound at the active site. The positions of the thymidine and  $\alpha$  and  $\beta$  phosphates with respect to the proteins are identical to the dTDP-D-glucose and dTDP-D-xylose complexes of *S. suis*. However, the carbohydrate rings are placed differently with respect to the protein because in the *P. aeruginosa* RmlC-product complex the nucleotide is equatorial to the carbohydrate ring not axial as in the *S. suis* complexes (Figure 2(c)). The C6' of the product is located in a hydrophobic region formed by F123 and G122. NZ of K74 and ND1 of H121 are coplanar with the sugar ring, and NZ of K74 hydrogen bonds (2.9  $\text{\AA}$ ) to the O4', the location of the negative charge in the enolate. Unlike the *S. suis* RmlC complexes, this interaction of O4' with the conserved Lys is now optimal for enolate stabilization (Figure 2(c)). H65 and Y134 of *P. aeruginosa* RmlC are located on opposite sides of the plane of the carbohydrate ring, entirely consistent with their identification as the



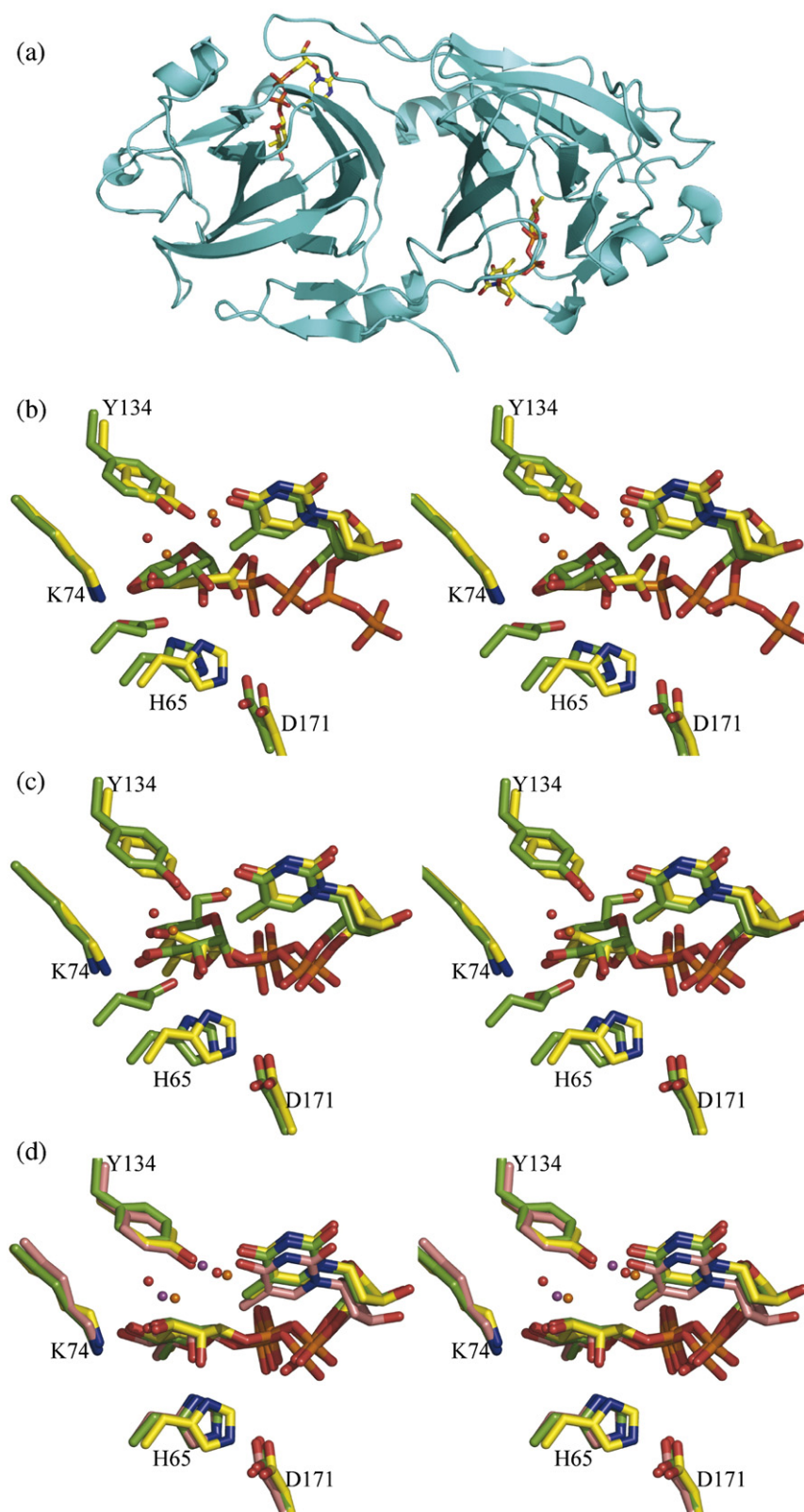


**Figure 2.** (a) Ribbon diagram of RmlC dimer from *P. aeruginosa* in complex with product (dTDP-6-deoxy-L-lyxo-4-hexulose). The product (an equatorially configured sugar nucleotide) is drawn in stick representation. The ligand atoms are shown in stick representation, with carbon yellow, nitrogen blue, oxygen red and phosphorus orange. (b) Superposition of the dTDP-D-xylose complex with RmlC from *P. aeruginosa* and from *S. suis*.<sup>19</sup> The  $\beta$  phosphate of dTDP-D-xylose in the *P. aeruginosa* is twisted out of the active site and a tartrate molecule occupies the active site in one monomer. In the *S. suis* structure the carbohydrate occupies the active site but is bound to E78 (shown but not labeled), a non-conserved residue on a loop not found in any other RmlC structure. The color scheme for *P. aeruginosa* complex is as in (a). For *S. suis* carbon atoms are colored green, other atoms are colored as for *P. aeruginosa*. Water molecules in the *P. aeruginosa* complex are shown as orange spheres, in the *S. suis* they are shown as red spheres. Amino acid numbering is for the *P. aeruginosa* sequence. (c) Superposition of the dTDP-6-deoxy-L-lyxo-4-hexulose (product) complex with RmlC from *P. aeruginosa* and the dTDP-glucose complex from *S. suis*.<sup>19</sup> Although the carbohydrate is bound at the active site in both complexes, the equatorial linkage between sugar and nucleotide in the *P. aeruginosa* complex means the sugar ring is positioned differently with respect to the key catalytic residues. The *P. aeruginosa* complex aligns better to the proposed chemical role of the active site residues. The color scheme is as in (b). The O6' of dTDP-D-glucose from *S. suis* replaces one of the conserved structural water molecules and is bound by E78 (shown but not labeled). Amino acid numbering is for the *P. aeruginosa* sequence. (d) Superposition of the dTDP-L-rhamnose complexes for three enzymes from *M. tuberculosis*, *S. suis* and *P. aeruginosa*. The match between the structures is particularly striking especially given the different crystallization conditions and low sequence identity

between the structures (25%). Two water molecules, one close to C3' and one close to C5', are structurally conserved. The *S. suis* and *P. aeruginosa* structure are colored as (c). The carbon atoms in *M. tuberculosis* RmlC complex are colored pink; other atoms are colored as for *P. aeruginosa*. The two water molecules in the *M. tuberculosis* structure are shown as magenta colored spheres. Amino acid numbering is for the *P. aeruginosa* sequence.

acid-base pair. The distances from OH of Y134 to C3' and C5' are 2.2 Å and 3.7 Å, respectively. Despite the close contact between the Y134 and C3', the electron

density does not suggest a full covalent link and may result from our failure to model any isomerization of keto group from the C4' to C3' position of the

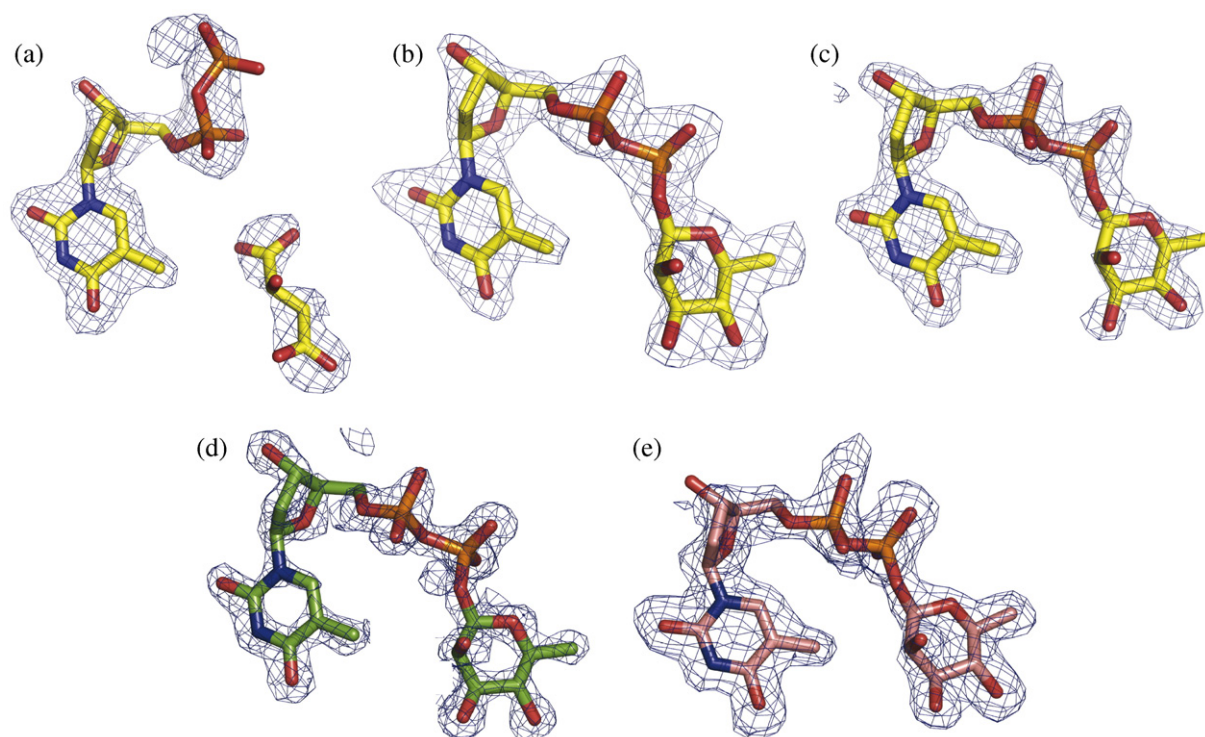


**Figure 3.** (a) Density from initial  $F_o-F_c$  map contoured at  $2.5\sigma$  for the *P. aeruginosa* RmlC complex with dTDP-D-xylose. The sugar is disordered and tartrate is seen at the active site of one subunit (shown here). Atoms are colored as in Figure 2(a). (b) Density from initial  $F_o-F_c$  map contoured at  $2.5\sigma$  for the *P. aeruginosa* RmlC complex with dTDP-6-deoxy-L-lyxo-4-hexulose. Atoms are colored as in Figure 2(a). (c) Density from initial  $F_o-F_c$  map contoured at  $2.5\sigma$  for the *P. aeruginosa* RmlC complex with dTDP-L-rhamnose. Atoms are colored as in Figure 2(a). (d) Density from initial  $F_o-F_c$  map contoured at  $2.5\sigma$  for the *S. suis* RmlC complex with dTDP-L-rhamnose. Carbon atoms are colored green, other atoms are colored as in Figure 2(a). Two subunits have clear density, in the other two the sugar component is significantly more disordered. (e) Density from initial  $F_o-F_c$  map contoured at  $2.5\sigma$  for the *M. tuberculosis* RmlC complex with dTDP-L-rhamnose. Carbon atoms are colored pink; other atoms are colored as in Figure 2(a). The quality of the density varies between subunits, with two being excellent, one weak and the fourth poor. In the subunit with weak density there is evidence for a second conformation of the sugar but we were unable to satisfactorily model it.

ring. In solution there is an equilibrium between dTDP-keto-sugar C4' and C3' keto groups.<sup>25</sup> However, the resolution of the data is insufficient to accurately model such an isomerization. The distances between the sugar C3'/C5' and ND1 of H65 are 3.4/3.6 Å (Figure 2(c)) and are consistent with H65 acting as the base for both C3' and C5' epimerization. This complex suggests that Y134 could act as the acid for both C3' and C5'. However, on the same face of the carbohydrate as the Tyr residue there are two water molecules that could also be involved in this process. One water molecule is located close to C5' and the other close to C3' (Figure 2(c)). In the dTDP-D-glucose complex with the *S. suis* protein, the water molecule close to C3' is preserved but the water close to C5' is displaced by the O6' of glucose (Figure 2(c)).

#### RmlC with dTDP-L-rhamnose

To further probe the recognition of an equatorial linked sugar, we employed dTDP-L-rhamnose as a product mimic. It differs from the authentic product in the reduction of the C4'-keto group to a hydroxyl

group. It was straightforward to obtain dTDP-L-rhamnose complexes with *P. aeruginosa*, *M. tuberculosis* and *S. suis* RmlC (Figure 3(c)–(e)). In all three complexes, the ligand and the key catalytic residues superimpose (Figure 2(d)). Comparison of the dTDP-L-rhamnose complex with the product complex from RmlC of *P. aeruginosa* revealed that the Tyr residue and the sugar ring have moved apart, resulting in a more normal 3.3 Å separation between C3' and the OH of Y134 and a 4.5 Å separation between C5' and the OH of Y134. Otherwise, the product and dTDP-L-rhamnose structures are essentially identical. The structural data suggest Tyr as the protein residue acting as the acid in both epimerizations. However, all three dTDP-L-rhamnose complexes also have the two water molecules at the same positions as seen in the product complex (Figure 2(d)). The consistency between these complexes is convincing, particularly given the differences in protein sequence and crystallization conditions. It also stands in marked contrast to our difficulties in obtaining dTDP-D-glucose or dTDP-D-xylose complexes with any RmlC protein except that from *S. suis*.



## Biochemical characterization

We have already reported assays of RmlC from *S. suis*<sup>19</sup> in which the key catalytic residues have been mutated. The conventional biochemical assay measures the amount of NADH consumed by RmlD in a coupled system and, therefore, only detects complete product formation by RmlC. This assay cannot be used to probe the individual steps in the reaction. In contrast, deuterium isotope incorporation directly measures the exchange of the protons at C3' and C5'. This exchange occurs when protons are abstracted from the substrate by a base and replaced by deuterons. While epimerization usually involves exchange, exchange can occur without epimerization.<sup>26</sup> This is the case here as, whilst there is a measurable background (uncatalyzed) rate of proton exchange at C3' and C5' of dTDP-6-deoxy-D-xylo-4-hexulose in <sup>2</sup>H<sub>2</sub>O, there is no observable uncatalyzed epimerization. The position and extent of deuterium incorporation from solvent can be assessed by analysis of GC-MS fragmentation patterns of alditol peracetates following reduction-hydrolysis-reduction-acetylation of dTDP-6-deoxy-D-xylo-4-hexulose and products of RmlC action<sup>27</sup> (Figure 4). In order to correct for non-enzymatic deuterium incorporation, two no-enzyme controls were performed at pH 5.0 and pH 9.0, respectively. The point mutants H63A, K73A and Y133F of RmlC from *S. enterica* serovar Typhimurium (corresponding to H65, K74, and Y134 from *P. aeruginosa* RmlC) were analyzed both for activity and for their ability to catalyze deuterium incorporation into the C3' and C5' positions of dTDP-6-deoxy-D-xylo-4-hexulose (Table 2 and Figure 4). The mutants were examined by circular dichroism, which confirmed no detectable structural changes that would influence the native fold. H63A is catalytically inactive and shows no deuterium incorporation above background at either C3' or C5'. K73A is reduced in activity by over 100-fold and a small amount of enzyme catalyzed deuterium incorporation was observed at C5', while only background levels were seen at C3'. This suggests that for the K73A mutant, C5' exchange is more rapid than at C3'. The catalytic activity of the Y133F mutant is reduced 1000-fold but shows some deuterium incorporation at C3' but none at C5' (above background). This indicates that RmlC can catalyze exchange of the proton at C3' without Tyr133 but not at C5'. While this assay measures proton/deuterium exchange rather than epimerization, it is possible that a small amount of C3' mono-epimerized product is produced by Y133F. In order to probe the different rates of exchange at the two positions, deuterium incorporation catalyzed by wild-type *S. enterica* serovar Typhimurium RmlC was monitored over a 30 min period at 10 °C. The rate of C5' incorporation is more rapid than at C3' (Figure 4). These data support a hypothesis that the dominant order of enzyme catalyzed exchange is generally C5' followed by C3'. The data do not exclude the possibility that exchange also occurs first at C3' followed by C5', but the data indicate that this

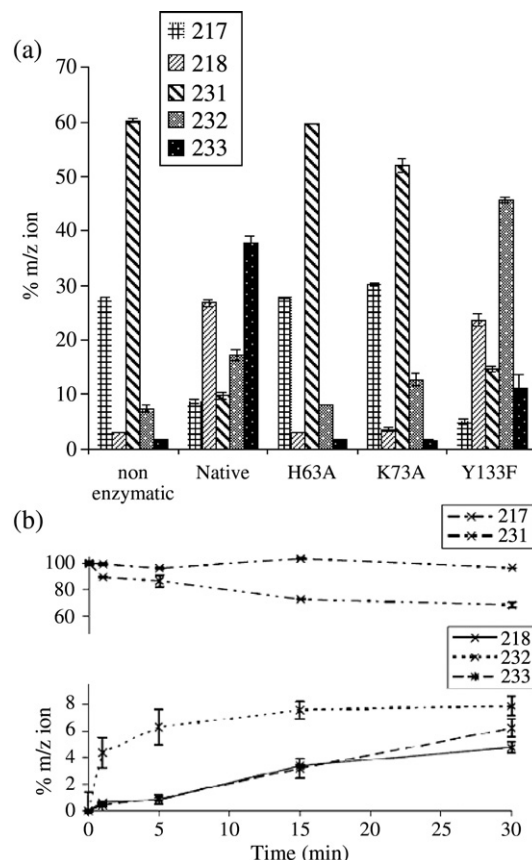


**Figure 4.** (a) Deuterium incorporation data for mutants of *S. enterica* serovar Typhimurium RmlC. The masses reflect the fragments of alditol per-acetates associated with deuterium incorporation into substrate. Cleavage between C3' and C4' with retention of charge at C3' yielded an ion at *m/z* 217 (no deuterium incorporation) or *m/z* 218 (deuterium incorporation at C3'). Cleavage between C2' and C3' with retention of charge at C-3 yielded an ion at *m/z* 231 (no deuterium incorporation), *m/z* 232 (deuterium at C3' or C5') and *m/z* 233 (deuterium at C3' and C5'). Starting material (no deuterium incorporation) has two peaks at 217/231. Deuterium incorporation at C5' only has peaks at 217 and 232. Deuterium incorporation at C3' has two peaks at 218 and 232. Deuterium incorporation at both C3' and C5' has peaks at 218 and 233. Only the Y133F mutant shows any specific C3' incorporation. The H63A shows no incorporation, whilst K79A shows some incorporation at C5' but none at C3'. Y133F mutant shows some C3' incorporation but no C5' incorporation. (b) A time-course at 10 °C measuring C3' and C5' deuterium incorporation into substrate, showing loss of signals from non-deuterated substrate (217, 231) and the evolution of deuterium incorporation. The C5'-specific peak at 232 is rapidly established and complete within 10 min, the same time frame as loss of the substrate 231 peak. The 218 peak appears more slowly and at approximately the same rate as the 233 peak. This suggests that there is no significant amount of specific C3' incorporation on its own, rather that C3' incorporation occurs (within error) after C5' incorporation.

is a minor component. Although exchange and epimerization are distinct, the first step proton abstraction is common to both. Based on our exchange data in which proton abstraction from C5' is

more rapid, we suggest that the enzyme may favor an order of epimerization with C5' first. Isothermal titration calorimetry shows quite clearly that dTDP-rhamnose (Figure 5) and dTDP are bound with a significantly higher affinity than dTDP-glucose and dTDP-xylose (Table 3). Whether there is a real difference between dTDP and dTDP-L-rhamnose binding cannot be reliably derived from the data that we have. The polar nature of sugars means that the hydrogen bonds they make with proteins are often cancelled by the ones they break with water. It seems likely that binding will be dominated by the nucleotide portion of the ligand. There are many examples of thermodynamically weak sugar protein interactions which have multiple hydrogen bonds.<sup>28,29</sup>

## Discussion

The RmlC reaction must proceed from substrate to a mono-epimerized intermediate, and subsequently

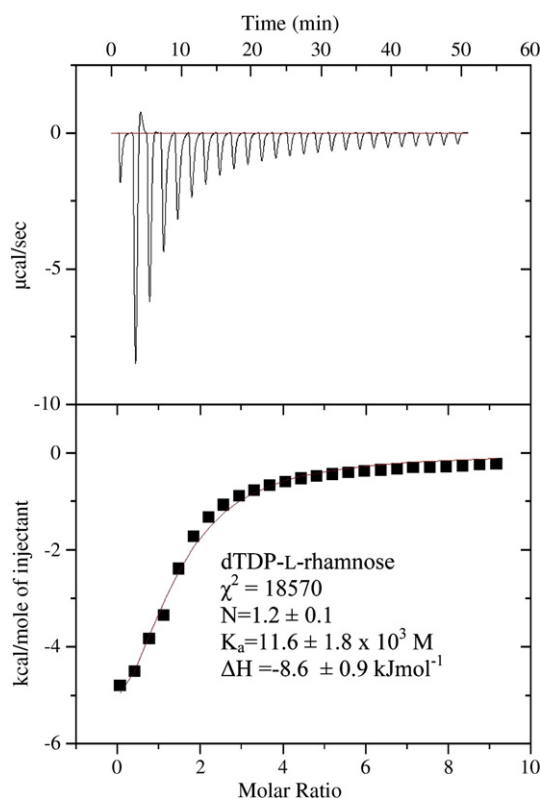


**Figure 5.** Raw isothermal titration calorimetry data for dTDP-L-rhamnose binding to *P. aeruginosa* RmlC. The small endothermic contribution in the second injection appears to be a consistent feature in three different experiments.  $\chi^2$  is a measure of the goodness of fit,  $N$  is the stoichiometry,  $K_a$  is the association constant and  $\Delta H$  is the enthalpy change. The concentration of the sugar was estimated by extinction coefficient. Fixing the stoichiometry to be 1:1 gives a  $K_a$  value of  $9.0 \times 10^3$  M. Eliminating the endothermic point from the fitting routine gives a stoichiometry of 1.04 and  $K_a$  of  $10 \times 10^3$  M. Eliminating the endothermic point and setting stoichiometry to 1 gives a  $K_a$   $9.7 \times 10^3$  M. Thus the value of  $K_a$  is robustly estimated from the data.

to a doubly epimerized product (Figure 1(a)). Our data suggest that the dominant order of epimerization may be C5' followed by C3' and our discussion focuses on this pathway. Our data do not exclude the possibility that there is no obligate order and that C3' epimerization can occur first. GME does exhibit a preference for C5' followed by C3' (Figure 1(b)). Structural and biochemical data are both consistent with an RmlC mechanism in which both the C5' and C3' protons are abstracted by the absolutely conserved His65 residue (*P. aeruginosa* numbering), which is part of a His-Asp dyad. Y134 has been shown to be essential for epimerization and for deuterium incorporation at C5'. This supports our proposal that Y134 has a key role in proton donation to C5' on the opposite face of the sugar to H65. Y134 is not essential for deuterium incorporation at C3' and water may be able to compensate for its absence during deprotonation but not during epimerization. In our structural analysis we noted a conserved water molecule close to the position appropriate for donation of a proton to C3'; this may partly compensate for the Tyr. NovW, a validated C3' mono-epimerase involved in novobiocin biosynthesis also acts on dTDP-6-deoxy-D-xylo-4-hexulose, retains the key active site Tyr residue despite conducting no chemistry at C5'.<sup>30</sup> The use of a His-Tyr couple is quite unusual in acid base enzyme chemistry. Histidine is, of course, widely used as both acid and base in many enzymes; GMER is thought to use a Cys-His<sup>23</sup> couple to carry out two epimerizations on sugar nucleotide. In catalyzing the dehydration of the C6' position, RmlB abstracts the same C5' proton as RmlC, but it uses a glutamic acid to accomplish this.<sup>31</sup> In amino acid racemases, which also remove a proton  $\alpha$  to a carbonyl group, a Cys-Cys couple is very commonly used.<sup>32</sup> Tyrosine is less widely used as base, although it is well known as the base in the short chain dehydrogenase superfamily<sup>33</sup> where it abstracts a hydroxyl proton. A tyrosine-water combination acts as one of the acid base groups during the racemization of alanine by *Treponema denticola* cystalysin; lysine acts as the other group.<sup>34</sup> Most recently and perhaps the most relevant to RmlC mechanism, the enzyme iminodisuccinate epimerase, which has a novel fold, has been predicted to use the a His-Tyr acid base couple and Lys to stabilize the enolate anion.<sup>35</sup> Proton abstraction from carbon by tyrosine is also seen in Chondroitin AC lyase.<sup>36</sup>

Structural data show that RmlC enzymes from *P. aeruginosa*, *M. tuberculosis* and *S. suis* recognize dTDP-L-rhamnose in an identical manner. This is in contrast to the situation with dTDP-D-glucose and dTDP-D-xylose. A product (dTDP-6-deoxy-L-lyxo-4-hexulose) complex obtained with *P. aeruginosa* RmlC confirms that dTDP-L-rhamnose is a very good product mimic. Isothermal titration calorimetry data establish that RmlC does bind dTDP-L-rhamnose more tightly than dTDP-glucose or dTDP-xylose (Table 3). We interpret these data to indicate that dTDP-L-rhamnose is more akin to the transition



state of the enzyme at the rate-determining step than either dTDP-xylose or dTDP-glucose. We suggest that the transition state has an equatorial linkage at the C1 position (dTDP-L-rhamnose) rather than an axial one (dTDP-xylose/glucose). This would tend to favor a mechanism in which the ring flip occurs as an integral part of catalysis rather than at the end (as has conventionally been written, Figure 1(a)). A ring flip at the end of epimerization would seem unlikely because the O1', C6' and O3' tri-axial clash would make the product very high in energy and presumably create a correspondingly high activation energy (Figure 6(a)). Structural studies on GME suggested that during the first epimerization at C5', the carbohydrate ring flips moving from an equatorial to axial linked carbohydrate.<sup>24</sup> This study experimentally established that a chair conformer with a C6' O1' diaxial clash is higher in energy than the ring flipped form which relieves such a strain. A similar process seems likely to occur in RmlC. We propose that as the proton is transferred to C5' by the Tyr, the carbohydrate ring flip occurs to give the equatorially linked sugar. If not, an axial C6' would be created by epimerization of the C5'; not only would this have the high energy C6' O1' diaxial interaction, but in addition C6' would severely clash with His. A major re-organization of the active site would be necessary to accommodate a non-ring-flipped mono-epimerized intermediate and in all the structure of RmlC, there is no evidence for such flexibility. By combining the ring flip with proton transfer the C6' remains fixed in space and avoids these very unfavorable interactions.

The ring-flipped intermediate poses a challenge for the enzyme for the second epimerization. The proton attached to C3' is not orthogonal to the plane of the carbonyl, as a result its  $pK_a$  is too high for removal by His.<sup>37</sup> As with GME,<sup>24</sup> there are two routes to create the required orthogonal arrangement of the  $\pi^*$  anti-bonding orbital of the carbonyl and  $\sigma$ -bonding orbital of the C3'. The ring could flip back to the high energy diaxial chair conformer that is conventionally written (Figure 1(a)). Alternatively, the keto group could move through the plane of the ring to give a twist boat (Figure 6(a)). We strongly favor the twist boat for three reasons. The diaxial chair conformer would seem to be very energetically unfavorable and it clashes with protein. In contrast there is good precedent from a variety of enzymes that twist boat structures are energetically accessible during enzyme catalysis.<sup>38</sup> Secondly, epimerization of the diaxial intermediate would create a transition state with some triaxial character. This is likely to be extremely unfavorable and have prohibitively high activation energy. Thirdly, the structural data and thermodynamics strongly support an optimized interaction between an equatorial-linked sugar nucleotide. The equatorial configuration at C1' is seen in the twist boat but not in the diaxial chair conformer.

It is possible that the substrate adopts a twist boat structure (Figure 6(b)). This could explain our apparent inability to obtain *P. aeruginosa* dTDP-

xylose complex in which the carbohydrate portion is located at the active site. The structure shows that the  $\beta$ -phosphate interaction with the protein is actually changed from that normally seen and thermodynamics establishes that the sugar binds much more weakly than dTDP-L-rhamnose. We suggest that the enzyme does not favor binding of the axially configured dTDP-xylose and as a result displaces the  $\beta$  phosphate from its normal binding site to position the sugar out of the active site. This would be consistent with the weaker binding of dTDP-glucose and dTDP-xylose relative to dTDP-L-rhamnose and dTDP (Table 3). As dTDP-D-xylose is smaller than the substrate (Figure 1(c)), non-binding cannot be explained by additional unfavorable steric clashes. Significantly, the dTDP-D-xylose and dTDP-D-glucose complexes of *S. suis*, which do locate an axially linked carbohydrate at the active site, do not superimpose with each other.<sup>39</sup> They also involve a key interaction with a non-conserved residue and are not optimally aligned for enolate stabilization. It may be that these complexes are artifacts of the *S. suis* enzyme. Despite differences in protein sequence, the three dTDP-L-rhamnose complexes, which have the equatorial linkage, superimpose with each other very well indeed and are properly aligned to the catalytic residues (Figure 4(d)). The substrate for RmlC has a C4' carbonyl group that will reduce the energy penalty for a twist boat structure by decreasing the C1', C4' diaxial interaction (Figure 6(b)). However, the twist boat, even for the keto sugar, will be higher in energy compared to the normal chair form of the substrate. This would require significant stabilization by the enzyme. The binding of the higher energy forms of carbohydrate substrate is well known from studies of other enzymes.<sup>40</sup> Further investigation will require sophisticated calculations that are beyond the scope of this work.

Despite having no similarity in sequence or structure, the chemical mechanisms of RmlC and GME are very similar. Both use a single amino acid as the catalytic base for both epimerizations, His in RmlC and Cys in GME. Both enzymes also seem to use a single amino acid as the proton source for both epimerizations, Lys in GME, Tyr in RmlC. In RmlC, water may be involved in C3' epimerization. Our data have provided the experimental evidence that supports a dominant order of C5' epimerization followed by C3' for both enzymes. The mono-epimerized intermediate in GME has been shown to be ring flipped (equatorial position for the nucleotide) and the structural data obtained here strongly suggest that this is also the case for RmlC. In both enzymes, the chemical requirements of the transformation to avoid unfavorable steric clashes, whilst activating the C3' proton for removal, indicate that the mono-epimerized intermediate adopts a twist boat character during catalysis. This convergence in mechanism from two quite different classes of enzyme appears to be driven by the unique chemistry of carbohydrate epimerization. The likely twist boat nature of the intermediate in the RmlC

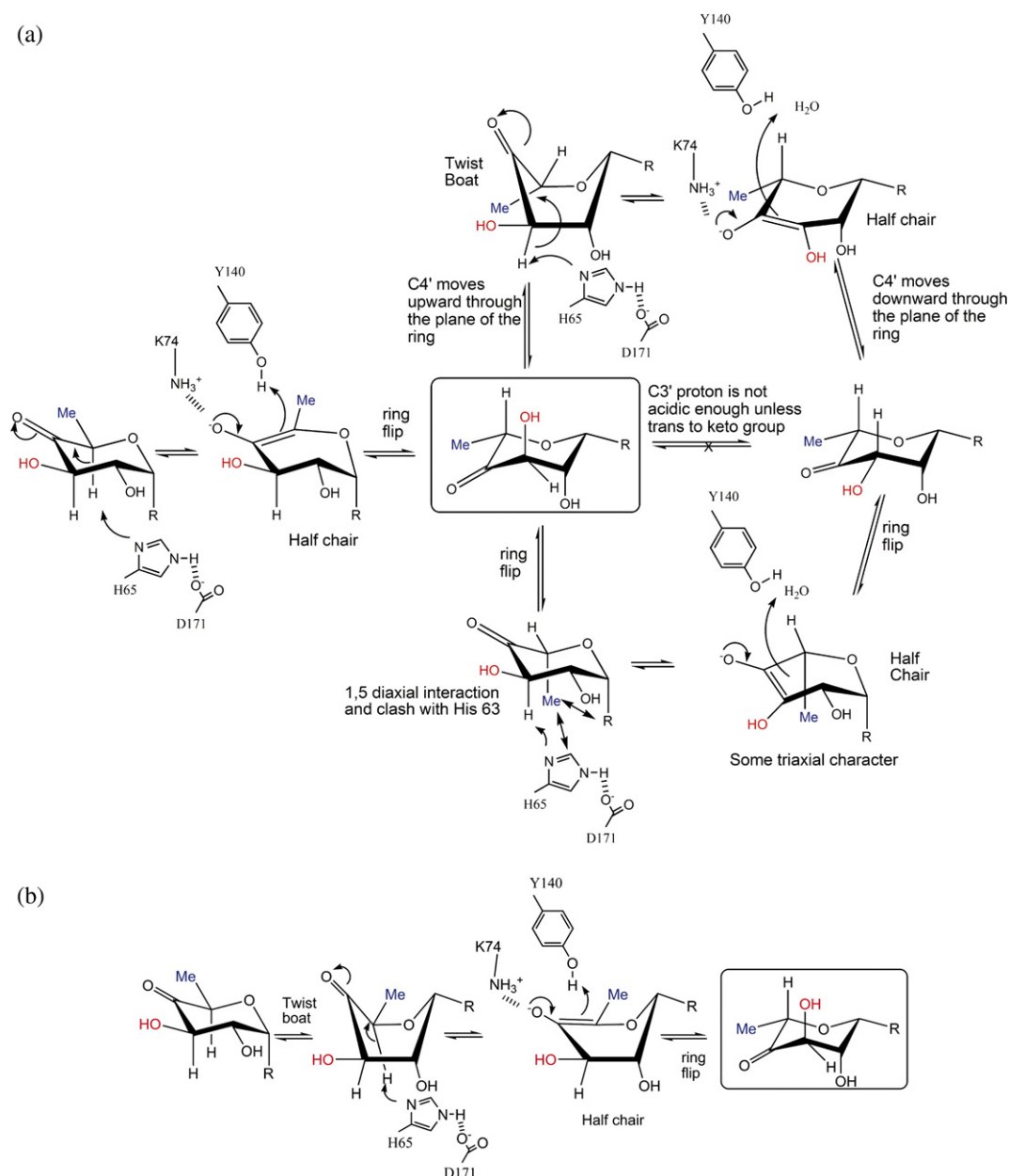


**Figure 6.** (a)  $R=OdTDP$ . A possible mechanism for RmlC based on structural and biochemical data. The key active site residues are shown, the H65 is the catalytic base for both epimerizations, K73 stabilizes the enolate and Y134 acts as the acid for the first epimerization. The mono-epimerized intermediate is shown boxed and has the equatorial linkage between carbohydrate ring and nucleotide. It cannot proceed directly to product because the C3' proton is only sufficiently acidic when it is orthogonal to the plane of the carbonyl function. (b)  $R=OdTDP$ . An alternative route for the first epimerization using a twist boat form of substrate, the mono epimerized intermediate is shown boxed. The apparent preference of RmlC for the equatorial linked sugar nucleotide suggests that this is a possibility.

mechanism will help guide inhibitor design against this validated drug target.

## Materials and Methods

### Protein expression and purification

The *rmlC* gene of *M. tuberculosis* strain H37Rv was cloned into pET23b using the Ligation Independent Clone system (Stratagene). The bacteria were grown in tryptone-phosphate medium until the  $A_{600\text{ nm}}$  reached 1.0, at which

time *rmlC* expression was induced by adding 1 mM IPTG and incubation was continued for 4 h. The protein was purified by elution from an anion exchange HQ column (Applied Biosystems) with an increasing NaCl gradient from 50 mM to 400 mM at pH 8.5 buffered with 20 mM Tris-HCl buffer. The second step was an elution from a hydrophobic exchange ET column (Applied Biosystems) with a decreasing 50% to 0% saturated ammonium sulfate gradient buffered at pH 7.3 by 20 mM phosphate. The purified protein was dialyzed against several changes of a solution containing 25 mM Tris-HCl buffer (pH 7.8) and concentrated to 7 mg ml<sup>-1</sup>. The *rmlC* gene of *P. aeruginosa* was cloned into pET23a(+) with an N-terminal 6× His tag

and a linker consisting of Gly-Ser-Met-Ala. The protein was overexpressed in *Escherichia coli* BL21 (DE3) cells grown in Luria broth medium. Once the  $A_{600\text{ nm}}$  reached 0.8, 1 mM IPTG was added and incubation was continued for 6 h. The protein was purified in a similar manner to *M. tuberculosis* RmlC; the principal difference was the use of a hydrophobic exchange HP column with a decreasing 25% to 0% saturated ammonium sulfate gradient. The protein was dialyzed against 25 mM Tris-HCl buffer (pH 7.8) and concentrated to 8 mg ml<sup>-1</sup>. The expression and purification of RmlC from *S. suis* has been described in detail<sup>19</sup> as has the protocol for RmlC from *S. enterica* serovar Typhimurium.<sup>15</sup> The purity of the proteins was determined by SDS-PAGE and their integrity by N-terminal sequencing, bioassays and MALDI-TOF mass spectrometry.

### Protein crystallization

The sugar nucleotides dTDP-rhamnose and dTDP-6-deoxy-D-xylo-4-hexulose were made enzymatically according to published procedures.<sup>41</sup> Crystals of *M. tuberculosis* RmlC (7 mg ml<sup>-1</sup>) complexed with dTDP-L-rhamnose were obtained in 23% (w/v) polyethylene glycol (PEG) 8000, 0.2 M calcium acetate hydrate, 0.1 M sodium cacodylate (pH 5.8). The protein was incubated with 10 mM dTDP-L-rhamnose overnight before crystallization; crystals took five to seven days to appear. Crystals of apo *P. aeruginosa* RmlC (7 mg ml<sup>-1</sup>) were grown in 10% PEG 8000, 0.2 M sodium tartrate, 0.1 M Mops (pH 6.5) and took two to three days to appear. Crystals of *P. aeruginosa* RmlC complexed with dTDP-L-rhamnose crystals were obtained in 20% PEG 8000, 0.2 M sodium tartrate, 0.1 M Mes (pH 5.8) with 10 mM dTDP-rhamnose after ten days. Crystals of *P. aeruginosa* RmlC complexed with product were obtained by incubating RmlC with 20 mM dTDP-6-deoxy-D-xylo-4-hexulose, for 2 h at room temperature, prior to setting up crystal plates with 25% PEG 8000, 0.2 M sodium tartrate, 0.1 M Mes (pH 6.2). With dTDP-D-xylose *P. aeruginosa* RmlC crystal conditions were changed to 25% PEG 8000, 0.2 M sodium tartrate, 0.1 M Mes (pH 6.4), 20 mM dTDP-xylose. All of the *P. aeruginosa* RmlC complex crystals grew to full size over 14 days. Crystals of *S. suis* RmlC in complex with dTDP-L-rhamnose (10 mM) were obtained from 25% PEG 2000, 0.1 M Tris-HCl (pH 7.6), 4 mM NiCl<sub>2</sub> after 14 days.

### Data collection and structural determination

Data to 1.7 Å resolution of *M. tuberculosis* RmlC in complex with dTDP-L-rhamnose were collected on SRS station 14.1 with an X-ray wavelength of 1.49 Å on an ADSC detector. *P. aeruginosa* apo RmlC data (2.5 Å) were collected in-house on a DIP2000 imaging plate system mounted on a Nonius rotating anode generator using CuKα radiation. Data for *P. aeruginosa* RmlC in complex with dTDP-rhamnose (2.0 Å), complexed with dTDP-xylose (1.8 Å), and for the *S. suis* RmlC dTDP-rhamnose complex (1.6 Å) were all collected at SRS station 9.6 with an X-ray wavelength of 0.86 Å on a MAR CCD detector. Data to 1.7 Å resolution were collected from crystals of *P. aeruginosa* RmlC in complex with product on ID14.2 at the ESRF. All data were processed and scaled using MOLSFLM<sup>42</sup> and SCALA.<sup>43</sup> Full details of data and refinement statistics are listed in Table 1. Structures were determined by molecular replacement using aMoRe<sup>44</sup> or

MOLREP,<sup>45</sup> using RmlC from *S. enterica* serovar Typhimurium as a model. Manual intervention was carried out in O.<sup>46</sup> Automated refinement of the structures used REFMAC5.<sup>47</sup> All structures were checked using PROCHECK.<sup>48</sup> Ligands were included in the models when the  $F_o - F_c$  electron density was clear at least one subunit (Figure 3).

### Biochemical characterization

Apparent  $K_m$  and  $k_{cat}$  measurements were made *via* a three-enzyme coupled assay described in detail previously<sup>41</sup> (Table 2). The assay monitors the consumption of NADH by RmlD under conditions where the concentration of RmlC is rate-limiting and thus the rate constants are apparent. Deuterium incorporation at C5' and/or C3' was also measured by an established protocol.<sup>27,49</sup> RmlC was mixed with ca 1 nmol dTDP-6-deoxy-D-xylo-4-hexulose in 30 µl of Hepes buffer (50 mM, pH 7.6) made up in <sup>2</sup>H<sub>2</sub>O for 2 h at 37 °C (Figure 4(a)) or at 10 °C for varying times for the time-course experiment (Figure 4(b)). The reaction was quenched by the addition of 50 µl of ethanol to precipitate protein, which was removed by centrifugation. NaBH<sub>4</sub> (2 mg) was then added to reduce both keto substrate and keto product at C4' to the hydroxyl group. This generates a mixture of four compounds as their dTDP adducts: 6-deoxy-D-glucose (quinovose) and 6-deoxy-D-galactose (fucose) from substrate, 6-deoxy-L-talose and 6-deoxy-L-mannose (rhamnose) from double epimerized product (to date, mono-epimerized products have not been detected in RmlC catalyzed reactions). Since the equilibrium position for the reactions lies very heavily in favor of substrate, the two former compounds dominate. Further, the borohydride reduction is stereoselective, giving the 6-deoxy-D-glucosyl configured product as the major isomer on steric grounds.<sup>50</sup> The samples were then hydrolyzed with trifluoroacetic acid, reduced with NaBH<sub>4</sub> (at C1') and acetylated to yield alditol acetates, which were analyzed by GC/MS. The  $m/z$  217, 218, 231, 232, and 232 ions of the dominant per-*O*-acetylated quinovositol peak (which was derived from the substrate) were quantified by GC-MS against an internal *myo*-inositol standard (Figure 4). The interpretation of the fragmentation pattern has been described elsewhere.<sup>27,49</sup> Briefly, cleavage between C3' and C4' with retention of charge at C3' yielded an ion at  $m/z$  217 (no deuterium incorporation at C3') or  $m/z$  218 (deuterium incorporation at C3'). Thus the presence of the 218 ion is definitive for C3' exchange and the presence of 217 for non exchange at C3'. Cleavage between C2' and C3' with retention of charge at C3' yielded an ion at  $m/z$  231 (no deuterium incorporation at either position),  $m/z$  232 (deuterium at either C3' or C5') and  $m/z$  233 (deuterium at C3' and C5'). Thus the presence of the ion at 233 is definitive for C3' and C5' exchange, the ion at 231 is definitive for no exchange at all. An ion at 232 accompanied by one at 217 but not 218 indicates C5' exchange in the absence of any C3' exchange, whereas ions at 218 and 232 but not 233, indicate C3' exchange in the absence of any C5' exchange.

The Promega GeneEditor site-directed mutagenesis kit was used to generate mutants of RmlC from *S. enterica* serovar Typhimurium with the following primers:

H63A, CTCAGAGGGCTAGCTTTTCAGAGAGGAG;  
K73A, GAAATGCACAGGGGGCGTTAGTTCGTTGTGC;  
and  
Y133F, GAGTTTCTGTTCAAAGCAAC.



**Table 1.** X-ray crystallographic data

	PA <sup>b</sup> apo	PA <sup>b</sup> product	PA <sup>b</sup> dTDP <sup>r</sup>	PA <sup>b</sup> dTDP <sup>x</sup>	MT <sup>b</sup> dTDP <sup>r</sup>	SS <sup>b</sup> dTDP <sup>r</sup>
Wavelength (Å)	1.54	0.933	0.87	0.87	1.488	0.87
Resolution (Å)	40.41–2.53	20.59–1.7	39.68–2.0	43.44–1.8	36.2–1.79	43–1.6
Highest shell	(2.67–2.53)	(1.79–1.70)	(2.11–2.0)	(1.9–1.8)	(1.89–1.79)	(1.69–1.60)
Cell dimension	$a=b=57.8$ $c=161.6$	$a=64.4$ $b=146.2$ $c=44.9$	$a=64.9$ $b=125.5$ $c=109.4$	$a=64.8$ $b=148.1$ $c=45.4$	$a=44.8$ $b=56.8$ $c=90.7$ $\alpha=89.9^\circ$ $\beta=82.3^\circ$ $\gamma=78.3^\circ$	$a=51.4$ $b=141.5$ $c=53.6$
Space group	$P4_12_12$	$P2_12_12$	$C222_1$	$P2_12_12$	$P1$	$P2_1$
Unique reflections	9710	40,067	30,581	35,190	84,823	99,569
Average redundancy	7.3 (6.3)	6.1 (4.7)	4.0 (4.0)	3.0 (3.1)	2.2 (2.2)	4.9 (4.1)
$I/\sigma$	6.8 (1.8)	5.6 (1.8)	6.3 (2.1)	5.5 (2.2)	7.5 (1.8)	6.6 (2.8)
Completeness (%)	99.2 (99.4)	84.3 (44.1)	99.9 (99.9)	80.1 (66.1)	92.6 (89.3)	99.1 (94.7)
$R_{\text{merge}}^a$ (%)	8.8 (41.9)	8.6 (38.4)	8.4 (35.6)	9.6 (34.9)	6.5 (29.9)	7.0 (24.8)
No of molecules in asymmetric unit	1	2	2	2	4	4
<i>Refinement</i>						
$R$ (%)	20.0 (31.9)	15.0 (17.4)	19.0 (24.5)	18.6 (21.7)	15.2 (18.3)	16.7 (17.8)
$R_{\text{free}}$ (5% of data) (%)	27.8 (44.7)	19.8 (25.3)	25.6 (29.2)	23.7 (28.8)	19.6 (25.9)	21.2 (27.4)
rmsd bonds (Å)/angles (°)	0.014/1.4	0.011/1.4	0.008/1.12	0.009/1.6	0.012/1.3	0.012/1.3
<i>B-factor deviation</i>						
Bonds/angles (Å <sup>2</sup> ):						
Main chain	0.6/1.0	1.3/1.5	0.5/0.6	0.7/0.7	0.9/1.2	0.9/1.2
Side-chains	1.5/2.3	2.2/3.1	0.9/1.3	1.2/1.9	1.9/2.6	1.8/2.5
Residues in Ramachandran core (%)	89	94	93	93	91	91
Protein atoms	1490	2982	2980	2992	6164	6335
Water atoms	92	531	590	455	1168	1383
dTDP ligand atoms	10	70	70	50 <sup>c</sup>	140	140
Protein average $B$ -factor (Å <sup>2</sup> )	26	15	35	20	26	12
Average $B$ -factor (Å <sup>2</sup> ) of dTDP-ligand	N/A	21	27	36 <sup>c</sup>	35	15
Average $B$ -factor (Å <sup>2</sup> ) waters	40	37	55	37	47	30
PDB accession code	2ixj	2ixk	2ixh	2ixi	2ixc	2ixl

<sup>a</sup>  $R_{\text{merge}} = \sum_{hkl} \sum_i |I_i - \langle I \rangle| / \sum_{hkl} \sum_i \langle I \rangle$ , where  $I_i$  is an intensity for the  $i$ th measurement of a reflection with indices  $hkl$  and  $\langle I \rangle$  is the weighted mean of the reflection intensity.

<sup>b</sup> PA, *P. aeruginosa*; MT, *M. tuberculosis*; SS, *S. suis*. DTDPR, dTDP-L-rhamnose; dTDPX, dTDP-D-xylose; dTDPR, dTDP-D-glucose.

<sup>c</sup> The carbohydrate portion of this ligand is partly disordered.

### Isothermal titration calorimetry

Titration experiments were performed in triplicate on a VP-ITC system (MicroCal) in 20 mM Tris-HCl base (pH 7.45). In a typical titration, 25 10  $\mu$ l injections of ligands (5 mM dTDP-L-rhamnose, dTDP-glucose and dTDP-xylose and 2 mM dTDP) were made into a solution *P. aeruginosa* RmlC (from 0.1 mM) in the ITC cell at 25 °C. Nucleotide concentrations were estimated by extinction coefficient. Control experiments were performed to assess the heat of dilution of each ligand by injecting this into buffer. There was no evidence of any self-association of the ligands (would be shown by a trend in the heats of dilution). Heats of dilution were subtracted from the original heats of interaction prior to data analysis. All

solutions were degassed prior to use. The resulting isotherms were fit using the ORIGIN software package (MicroCal). The data were fitted to the simplest model based on independent binding sites. The  $K_a$  values derived in Table 3 come from unrestrained refinement; fixing the stoichiometry ( $N$ ) to 1 does not change the value of  $K_a$  within error, except for dTDP. For dTDP fixing  $N=1$ , drops

**Table 3.** Isothermal titration calorimetry data for *P. aeruginosa* RmlC with sugar nucleotides

	$K_a$ ( $\times 10^3$ M)	$\Delta H$ (kJ mol <sup>-1</sup> )
dTDP-L-rhamnose	11.6 $\pm$ 1.8	-8.6 $\pm$ 0.9
dTDP <sup>a</sup>	13.2 $\pm$ 1.7	-25 $\pm$ 2
dTDP-xylose	1.32 $\pm$ 0.05	-11.8 $\pm$ 0.2
dTDP-glucose	0.96 $\pm$ 0.26	-9.3 $\pm$ 6.2

The uncertainties are estimated from the fitting and underestimate the true error.

<sup>a</sup> The values for dTDP did vary depending on experiment and on the processing parameters. As is seen for dTDP-L-rhamnose (Figure 5) there is an endothermic event at the start of titration that we cannot interpret. If the endothermic points are omitted,  $N$  is set to 1 and the values recalculated the  $K_a$  drops to  $4.5 \times 10^3$  M. Our interpretation is that dTDP binds more tightly than dTDP-xylose/glucose, we do not think our data robust enough to compare dTDP and dTDP-L-rhamnose.

**Table 2.** Apparent kinetic constants for *S. enterica* serovar Typhimurium RmlC mutants with dTDP-6-deoxy-D-xylo-4-hexulose

Enzyme	$K_m$ (mM)	$k_{\text{cat}}$ (1/s)
Native	0.71 $\pm$ 0.17	39 $\pm$ 6.6
RmlC K73A	0.35 $\pm$ 0.051	0.095 $\pm$ 0.0083
RmlC Y133F	0.48 $\pm$ 0.21	0.016 $\pm$ 0.0017
RmlC H63A	N.D	0

$K_a$  to  $10^3$  M. This does not change the interpretation of our data. No matter how  $K_a$  is calculated for dTDP, it is always significantly higher than dTDP-xylose/glucose. The same is true for dTDP-L-rhamnose: it binds significantly more tightly than dTDP-xylose/glucose. Whether dTDP-L-rhamnose binds significantly more tightly than dTDP (or within error equally tightly) does not affect our analysis and is a secondary issue. We do not believe the data that we have obtained reliably establish this. The errors in Table 3 are those derived from the fit, the impurity inherent in all sugar nucleotide preparations will increase the actual error of the experiment. For calorimetry we synthesized fresh dTDP-L-rhamnose enzymatically using 1.1 mM dTDP-D-glucose, 1.1  $\mu$ M *S. suis* RmlB, 0.4  $\mu$ M *S. enterica* serovar Typhimurium RmlC, 0.5  $\mu$ M *M. tuberculosis* RmlD, in 180 mM Tris-HCl (pH 7.5), 18 mM  $MgCl_2$ , 1.8 mM NADPH. Reaction mixtures were incubated for 90 min at 37 °C, then protein was removed from the mixture by centrifugation through an Amicon microcon 10 kDa molecular mass cut-off regenerated cellulose column. Compounds were separated on a Phenomenex Kingsorb 5  $\mu$  C-18 column (250 mm  $\times$  21.2 mm) at a flow rate of 8 ml min<sup>-1</sup>. The column was equilibrated with 20 mM triethylammonium acetate (TEAA) (pH 6.0) containing 3% acetonitrile prior to sample loading. After 5 min isocratic elution with 20 mM TEAA (pH 6.0) and 3% acetonitrile, compounds were eluted with a gradient of 3.0–3.7% acetonitrile over 30 min. Eluant was monitored by a UV detector at 267 nm. This procedure is based on a published method for purifying nucleotide sugars.<sup>51</sup> The dTDP-L-rhamnose peak eluted at approximately 3.4% acetonitrile and was collected, the mass of the major component confirmed as 547 by LCT-MS in negative ion mode and the compound freeze dried. dTDP-glucose and dTDP were purchased from FLUKA. dTDP-xylose was synthesized chemically by established methods.<sup>52</sup>

### Protein Data Bank accession codes

The atomic coordinates have been deposited with the RCSB Protein Data Bank and are available under accession codes as in Table 1.

### Acknowledgements

J.H.N. is a Career Development Fellow of Biotechnology and Biology Research Council (BBSRC). The work is supported by grants from the Wellcome Trust and NIH. C.W. and J.S.L. are Canada Research Chairs and acknowledge funding from the Natural Sciences Engineering Research Council and the Canadian Cystic Fibrosis Foundation, respectively. R.A.F. thanks the BBSRC and the EPSRC for financial support. We thank Wulf Blankenfeldt and Uli Schwartz-Linek for assistance and helpful discussions.

### Supplementary Data

Supplementary data associated with this article can be found, in the online version, at doi:10.1016/j.jmb.2006.09.063

### References

- Sharon, N. & Lis, H. (1989). Lectins as cell recognition molecules. *Science*, **246**, 227–233.
- Allard, S. T., Giraud, M. F. & Naismith, J. H. (2001). Epimerases: structure, function and mechanism. *Cell. Mol. Life Sci.* **58**, 1650–1665.
- Field, R. A. & Naismith, J. H. (2003). Structural and mechanistic basis of bacterial sugar nucleotide-modifying enzymes. *Biochemistry*, **42**, 7637–7647.
- Tanner, M. E. (2001). Sugar nucleotide-modifying enzymes. *Curr. Org. Chem.* **5**, 169–192.
- Ma, Y., Stern, R. J., Scherman, M. S., Vissa, V. D., Yan, W., Jones, V. C. *et al.* (2001). Drug targeting *Mycobacterium tuberculosis* cell wall synthesis: genetics of dTDP-rhamnose synthetic enzymes and development of a microtiter plate-based screen for inhibitors of conversion of dTDP-glucose to dTDP-rhamnose. *Antimicrob. Agents Chemother.* **45**, 1407–1416.
- Babaoglu, K., Page, M. A., Jones, V. C., McNeil, M. R., Dong, C. J., Naismith, J. H. & Lee, R. E. (2003). Novel inhibitors of an emerging target in *Mycobacterium tuberculosis*; substituted thiazolidinones as inhibitors of dTDP-rhamnose synthesis. *Bioorgan. Med. Chem. Letters*, **13**, 3227–3230.
- Mills, J. A., Motichka, K., Jucker, M., Wu, H. P., Uhlik, B. C., Stern, R. J. *et al.* (2004). Inactivation of the mycobacterial rhamnosyltransferase, which is needed for the formation of the arabinogalactan-peptidoglycan linker, leads to irreversible loss of viability. *J. Biol. Chem.* **279**, 43540–43546.
- Rahim, R., Burrows, L. L., Monteiro, M. A., Perry, M. B. & Lam, J. S. (2000). Involvement of the rml locus in core oligosaccharide and O polysaccharide assembly in *Pseudomonas aeruginosa*. *Microbiology*, **146**, 2803–2814.
- Tsukioka, Y., Yamashita, Y., Oho, T., Nakano, Y. & Koga, T. (1997). Biological function of the dTDP-Rhamnose synthesis pathway in *Streptococcus mutans*. *J. Bacteriol.* **179**, 1126–1134.
- Yamashita, Y., Tomihisa, K., Nakano, Y., Shimazaki, Y., Oho, T. & Koga, T. (1999). Recombination between *gtfB* and *gtfC* is required for survival of a dTDP-rhamnose synthesis-deficient mutant of *Streptococcus mutans* in the presence of sucrose. *Infect. Immun.* **67**, 3693–3697.
- Ma, Y., Pan, F. & McNeil, M. (2002). Formation of dTDP-rhamnose is essential for growth of mycobacteria. *J. Bacteriol.* **184**, 3392–3395.
- Melo, A. & Glaser, L. (1968). The mechanism of 6-deoxyhexose synthesis. II. Conversion of deoxythymidine diphosphate 4-keto-6-deoxy-D-glucose to deoxythymidine diphosphate L-rhamnose. *J. Biol. Chem.* **243**, 1475–1478.
- Blankenfeldt, W., Asuncion, M., Lam, J. S. & Naismith, J. H. (2000). The structural basis of the catalytic mechanism and regulation of glucose-1-phosphate thymidyltransferase (RmlA). *EMBO J.* **19**, 6652–6663.
- Allard, S. T., Giraud, M. F., Whitfield, C., Messner, P. & Naismith, J. H. (2000). The purification, crystallization and structural elucidation of dTDP-D-glucose 4,6-dehydratase (RmlB), the second enzyme of the dTDP-L-rhamnose synthesis pathway from *Salmonella enterica* serovar typhimurium. *Acta Crystallog. sect. D*, **56**, 222–225.
- Giraud, M. F., Leonard, G. A., Field, R. A., Bernlind, C. & Naismith, J. H. (2000). RmlC, the third enzyme of dTDP-L-rhamnose pathway, is a new class of epimerase. *Nature Struct. Biol.* **7**, 398–402.
- Blankenfeldt, W., Kerr, I. D., Giraud, M. F., McMiken,

- H. J., Leonard, G., Whitfield, C. *et al.* (2002). Variation on a theme of SDR. dTDP-6-deoxy-L-lyxo-4-hexulose reductase (RmlD) shows a new  $Mg^{2+}$ -dependent dimerization mode. *Structure*, **10**, 773–786.
17. Beis, K., Allard, S. T., Hegeman, A. D., Murshudov, G., Philp, D. & Naismith, J. H. (2003). The structure of NADH in the enzyme dTDP-D-glucose dehydratase (RmlB). *J. Am. Chem. Soc.* **125**, 11872–11878.
  18. Christendat, D., Saridakis, V., Dharamsi, A., Bochkarev, A., Pai, E. F., Arrowsmith, C. H. & Edwards, A. M. (2000). Crystal structure of dTDP-4-keto-6-deoxy-D-hexulose 3,5-epimerase from *Methanobacterium thermoautotrophicum* complexed with dTDP. *J. Biol. Chem.* **275**, 24608–24612.
  19. Dong, C. J., Major, L. L., Allen, A., Blankenfeldt, W., Maskell, D. & Naismith, J. H. (2003). High-resolution structures of RmlC from *Streptococcus suis* in complex with substrate analogs locate the active site of this class of enzyme. *Structure*, **11**, 715–723.
  20. Kantardjieff, K. A., Kim, C. Y., Naranjo, C., Waldo, G. S., Legin, T., Segelke, B. W. *et al.* (2004). *Mycobacterium tuberculosis* RmlC epimerase (Rv3465): a promising drug-target structure in the rhamnose pathway. *Acta Crystallog. sect. D*, **60**, 895–902.
  21. Rizzi, M., Tonetti, M., Vigevari, P., Sturla, L., Bisso, A., De Flora, A. *et al.* (1998). GDP-4-keto-6-deoxy-D-mannose epimerase/reductase from *Escherichia coli*, a key enzyme in the biosynthesis of GDP-L-fucose, displays the structural characteristics of the RED protein homology superfamily. *Structure*, **6**, 1453–1465.
  22. Menon, S., Stahl, M., Kumar, R., Xu, G. Y. & Sullivan, F. (1999). Stereochemical course and steady state mechanism of the reaction catalyzed by the GDP-fucose synthetase from *Escherichia coli*. *J. Biol. Chem.* **274**, 26743–26750.
  23. Somers, W. S., Stahl, M. L. & Sullivan, F. X. (1998). GDP-fucose synthetase from *Escherichia coli*: structure of a unique member of the short-chain dehydrogenase/reductase family that catalyzes two distinct reactions at the same active site. *Structure*, **6**, 1601–1612.
  24. Major, L. L., Wolucka, B. A. & Naismith, J. H. (2005). Structure and function of GDP-mannose-3',5'-epimerase: an enzyme which performs three chemical reactions at the same active site. *J. Am. Chem. Soc.* **127**, 18309–18320.
  25. Naundorf, A. & Klaffke, W. (1996). Substrate specificity of native dTDP-D-glucose-4,6-dehydratase: chemo-enzymatic syntheses of artificial and naturally occurring deoxy sugars. *Carbohydr. Res.* **285**, 141–150.
  26. Merkel, A. B., Major, L. L., Errey, J. C., Burkart, M. D., Field, R. A., Walsh, C. T. & Naismith, J. N. (2004). The position of a key tyrosine in dTDP-4-keto-6-deoxy-D-glucose-5-epimerase (EvaD) alters the substrate profile for this RmlC-like enzyme. *J. Biol. Chem.* **279**, 32684–32691.
  27. York, W. S., Darvill, A. G., Mcneil, M., Stevenson, T. T. & Albersheim, P. (1986). Isolation and characterization of plant-cell walls and cell-wall components. *Enzymol.* **118**, 3–40.
  28. Bryce, R. A., Hillier, I. H. & Naismith, J. H. (2001). Carbohydrate-protein recognition: molecular dynamics simulations and free energy analysis of oligosaccharide binding to concanavalin A. *Biophys. J.* **81**, 1373–1388.
  29. Moothoo, D. N., Canan, B., Field, R. A. & Naismith, J. H. (1999). Man  $\alpha$ 1-2 Man  $\alpha$ -OMe-concanavalin A complex reveals a balance of forces involved in carbohydrate recognition. *Glycobiology*, **9**, 539–545.
  30. Tello, M., Jakimowicz, P., Errey, J. C., Meyers, C. L. F., Walsh, C. T., Buttner, M. J. *et al.* (2006). Characterisation of *Streptomyces spheroides* NovW and revision of its functional assignment to a dTDP-6-deoxy-D-xylo-4-hexulose 3-epimerase. *Chem. Commun.*, 1079–1081.
  31. Allard, S. T., Beis, K., Giraud, M. F., Hegeman, A. D., Gross, J. W., Wilmouth, R. C. *et al.* (2002). Toward a structural understanding of the dehydratase mechanism. *Structure*, **10**, 81–92.
  32. Williams, G., Maziarz, E. P., Amyes, T. L., Wood, T. D. & Richard, J. P. (2003). Formation and stability of the enolates of N-protonated proline methyl ester and proline zwitterion in aqueous solution: a nonenzymatic model for the first step in the racemization of proline catalyzed by proline racemase. *Biochemistry*, **42**, 8354–8361.
  33. Jornvall, H., Persson, B., Krook, M., Atrian, S., Gonzalez-Duarte, R., Jeffery, J. & Ghosh, D. (1995). Short-chain dehydrogenases/reductases (SDR). *Biochemistry*, **34**, 6003–6013.
  34. Cellini, B., Bertoldi, M., Paiardini, A., D'Aguanno, S. & Voltattorni, C. B. (2004). Site-directed mutagenesis provides insight into racemization and transamination of alanine catalyzed by *Treponema denticola* cystalysin. *J. Biol. Chem.* **279**, 36898–36905.
  35. Lohkamp, B., Bäuerle, B., Rieger, P.-G. & Schneider, G. (2006). Three-dimensional structure of iminodisuccinate epimerase defines the fold of the MmgE/PrpD protein family. *J. Mol. Biol.* **362**, 555–566.
  36. Rye, C. S., Matte, A., Cygler, M. & Withers, S. G. (2006). An atypical approach identifies TYR234 as the key base catalyst in chondroitin AC lyase. *ChemBiochem*, **7**, 631–637.
  37. Corey, E. J. (1954). The stereochemistry of -haloketones V. Prediction of the stereochemistry of -brominated ketosteroids. *J. Am. Chem. Soc.* **76**, 175–179.
  38. Vasella, A., Davies, G. J. & Matthias, B. (2002). Glycosidase mechanisms. *Trends Chem. Biol.* **6**, 619–629.
  39. Dong, C., Major, L. L., Allen, A., Blankenfeldt, W., Maskell, D. & Naismith, J. H. (2003). High-resolution structures of RmlC from *Streptococcus suis* in complex with substrate analogs locate the active site of this class of enzyme. *Structure*, **11**, 715–723.
  40. Sinnott, M. L., Guo, X. M., Li, S. C. & Li, Y. T. (1993). Leech sialidase-L cleaves the glycon aglycon bond with the substrate in a normally disfavored conformation. *J. Am. Chem. Soc.* **115**, 3334–3335.
  41. Graninger, M., Nidetzky, B., Heinrichs, D. E., Whitfield, C. & Messner, P. (1999). Characterization of dTDP-4-dehydrorhamnose 3,5-epimerase and dTDP-4-dehydrorhamnose reductase, required for dTDP-L-rhamnose biosynthesis in *Salmonella enterica* serovar Typhimurium LT2. *J. Biol. Chem.* **274**, 25069–25077.
  42. Leslie, A. G. W. (1992). Recent changes to the MOSFLM package for processing film and image plate data. *Joint CCP4 and ESF-EAMCB Newsletter Protein Crystallog.* **26**, 1–10.
  43. Bailey, S. (1994). The Ccp4 Suite - programs for protein crystallography. *Acta Crystallog. sect. D*, **50**, 760–763.
  44. Navaza, J. (1994). AMoRe: an automated package for molecular replacement. *Acta Crystallog. sect. A*, **50**, 157–163.
  45. Vagin, A. & Teplyakov, A. (1997). MOLREP: an automated program for molecular replacement. *J. Appl. Crystallog.* **30**, 1022–1025.
  46. Jones, T. A., Zou, J.-Y., Cowan, S. W. & Kjeldgaard, M. (1991). Improved methods for building protein models in electron density maps and the location of errors in these models. *Acta Crystallog. sect. A*, **47**, 110–119.



47. Murshudov, G. N., Vagin, A. A., Lebedev, A., Wilson, K. S. & Dodson, E. J. (1999). Efficient anisotropic refinement of macromolecular structures using FFT. *Acta Crystallog. sect. D*, **55**, 247–255.
48. Laskowski, R. A., MacArthur, M. W., Moss, D. S. & Thornton, J. M. (1993). PROCHECK: a program to check the stereochemical quality of protein structures. *J. Appl. Crystallog.* **26**, 548–558.
49. Kirkpatrick, P. N., Scaife, W., Hallis, T. M., Liu, H., Spencer, J. B. & Williams, D. H. (2000). Characterisation of a sugar epimerase enzyme involved in the biosynthesis of a vancomycin-group antibiotic. *Chem. Commun.*, 1565–1566.
50. Stern, R. J., Lee, T. Y., Lee, T. J., Yan, W., Scherman, M. S., Vissa, V. D. *et al.* (1999). Conversion of dTDP-4-keto-6-deoxyglucose to free dTDP-4-keto-rhamnose by the rmlC gene products of *Escherichia coli* and *Mycobacterium tuberculosis*. *Microbiology*, **145**, 663–671.
51. Järvinen, N., Mäki, M., Rabinä, J., Roos, C., Mattila, P. & Renkonen, R. (2001). Cloning and expression of *Helicobacter pylori* GDP-L-fucose synthesizing enzymes (GMD and GMER) in *Saccharomyces cerevisiae*. *Eur. J. Biochem.* **268**, 6458–6464.
52. Ballell, L., Young, R. J. & Field, R. A. (2005). Synthesis and evaluation of mimetics of UDP and UDP-alpha-D-galactose, dTDP and dTDP-alpha-D-glucose with monosaccharides replacing the key pyrophosphate unit. *Org. Biomol. Chem.* **3**, 1109–1115.

*Edited by I. Wilson*

(Received 6 June 2006; received in revised form 21 September 2006; accepted 22 September 2006)  
Available online 29 September 2006